

# Coaxial Electrospray Formulations for Improving Oral Absorption of a Poorly Water-Soluble Drug

Shaoling Zhang,<sup>†</sup> Kohsaku Kawakami,<sup>\*,†,‡</sup> Marina Yamamoto,<sup>§</sup> Yoshie Masaoka,<sup>§</sup> Makoto Kataoka,<sup>§</sup> Shinji Yamashita,<sup>§</sup> and Shinji Sakuma<sup>\*,§</sup>

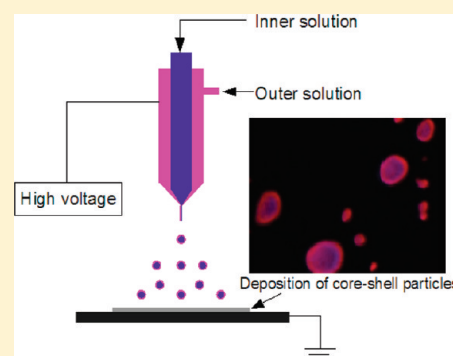
<sup>†</sup>Biomaterials Center, National Institute for Materials Science, Tsukuba 305-0044, Japan

<sup>‡</sup>International Center for Materials Nanoarchitectonics, Tsukuba 305-0044, Japan

<sup>§</sup>Faculty of Pharmaceutical Sciences, Setsunan University, 45-1 Nagaotoge-cho, Hirakata, Osaka 573-0101, Japan

**ABSTRACT:** Development of oral dosage forms containing poorly water-soluble drugs is a major challenge in the pharmaceutical industry. This paper describes the use of coaxial electrospray deposition as a promising formulation technology for oral delivery of poorly water-soluble drugs. The technology produced core-shell particles composed of griseofulvin and poly(methacrylic acid-co-methyl methacrylate) (Eudragit L-100), with a diameter of around 1  $\mu\text{m}$ . The drug phase was in an amorphous state when the griseofulvin core was coated with the Eudragit L-100 shell. The *in vitro* dissolution and *in vivo* oral absorption studies revealed that the core-shell formulation significantly improved dissolution and absorption behaviors, presumably because of a reduction in particle size, improvement in dispersity, and amorphization. Results demonstrated that coaxial electrospray deposition possesses great potential as novel formulation technology for enhancing oral absorption of poorly water-soluble drugs.

**KEYWORDS:** griseofulvin, amorphous, electrospray deposition, core-shell particle, poorly water-soluble drug



## INTRODUCTION

Over the past decade, there has been much discussion on favorable physicochemical properties for drug candidates.<sup>1–4</sup> Nevertheless, formulators must still deal with many challenging compounds including poorly water-soluble ones. Various special dosage forms including self-emulsifying drug delivery systems,<sup>5–8</sup> solid dispersions,<sup>9–12</sup> and nanocrystals<sup>13–16</sup> have been actively developed for overcoming the solubility problem. Although development and manufacturing of self-emulsifying drug delivery systems are relatively simple, it tends to offer inconvenient formulation due to its large volume and strict storage conditions.<sup>17</sup> On the other hand, solid dispersions and nanocrystals are free from such inconveniences so that they can be taken as simple tablets or capsules. However, there are still limited numbers of marketed solid dispersions and nanocrystals, mainly because of their physical stability and manufacturing problems.<sup>17</sup>

Electrospray deposition is a novel versatile technique and has been applied to micro/nanofabrication of various materials.<sup>18,19</sup> Although the drug delivery field is regarded as one of the promising application areas,<sup>20–23</sup> the advantage of this method has hardly been revealed in *in vivo* studies. Various characteristics, including sustained release and enhanced dissolution rate, are expected for the electrospray formulation, depending on morphology of the formulation and the characteristics of the excipients used. Although the former has already been achieved,<sup>20,21</sup> the latter should suffer from the aggregation problem, which is a universal concern for any solid nanoparticulate systems. A coaxial electrospray technology<sup>24–28</sup> may solve this problem because it

provides core-shell particles with surface modification. In addition to the nanofabrication ability, the electrospray method is regarded as an amorphization technique as well. Industrial production of the oral amorphous formulation is usually achieved by hot melt extrusion or spray-drying, both of which require thermal stress. The great advantage of the electrospray method is that it can be operated at ambient temperature and pressure conditions. The electrospray formulation is expected to improve dissolution of poorly water-soluble drugs with two mechanisms: nanosizing and amorphization.

Griseofulvin (GF) is an oral effective antifungal agent with poor solubility and low bioavailability. Since the rate-limiting step of the oral absorption of GF is the dissolution process, bioavailability can be improved by technologies for increasing the dissolution rate including micronization and amorphization. Therefore, the electrospray technology was expected to overcome the solubility problem of GF. In this study, GF was coaxially electrosprayed with Eudragit L-100, and the effectiveness of the electrospray technology was investigated. Eudragit L-100 is an anionic polymer synthesized from methacrylic acid and methyl methacrylate. It has a pH dependent solubility and is widely used as coating material of oral formulations. It was used as material for shell of the particulate formulation.

**Received:** November 24, 2010

**Accepted:** March 11, 2011

**Revised:** February 3, 2011

**Published:** March 11, 2011

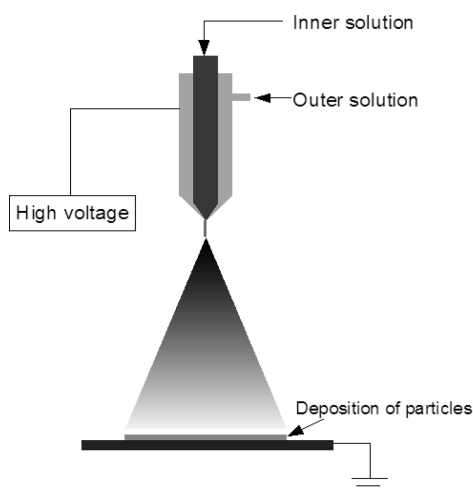


Figure 1. Illustration of the coaxial electrospray setup.

## EXPERIMENTAL SECTION

**Materials.** Griseofulvin (GF) and poly(methacrylic acid-co-methyl methacrylate), which is commonly called Eudragit L100 (L-100), were obtained from Wako Pure Chemical (Osaka, Japan) and Rohm Pharma GmbH (Darmstadt, Germany), respectively. Coumarin, Rhodamine B and taurocholic acid sodium salt were purchased from Nacalai Tesque (Kyoto, Japan). All chemicals were used without further purification.

**Preparation of Formulations.** Crystalline GF, physical mixture (PM) of GF and L-100, and two coaxial electrospray formulations were investigated in this study. Crystalline GF was ground with a mortar and pestle prior to the studies. PM was prepared by mixing GF and L-100 at a 1:4 mass ratio in a mortar and pestle.

The coaxial electrospray setup is shown in Figure 1. In order to obtain particles of a narrow size distribution, and to operate the system in the cone-jet mode, the solution and processing parameters were optimized on the basis of a systematic investigation reported previously.<sup>29</sup> Solution conductivity and viscosity were shown as the most important parameters for stable operation. Although high viscosity was favored from the viewpoint of stable operation, increase in the polymer concentration led to increase in the particle size. Thus, L-100 and GF were dissolved in ethanol and chloroform, respectively, at a concentration of 10 g/L, which was found to be optimum from both viewpoints. Conductivity of these two solutions was 8.98 and 0.09  $\mu\text{S}/\text{cm}$ , respectively. In this study, control of conductivity was not necessary, since it was always sufficiently low regardless of the type of solvent and the concentration. The solutions were supplied by syringe pumps to the coaxial nozzle, to which a high positive voltage of 25 kV was applied. The flow rate was determined by considering particle size and the productivity. The inner and outer nozzle diameters were 0.4 and 0.8 mm, respectively. A grounded steel plate was placed perpendicular to the nozzle as a deposition target. The distance between the nozzle and the target was 15 cm. The electrospray was conducted in an acrylic chamber at ambient temperature. The humidity was controlled at lower than 20% RH by flowing nitrogen gas.

For entrapping GF by L-100 and obtaining core-shell structure,<sup>27</sup> the GF chloroform solution was used inside and the L-100 ethanol solution outside, with flow rates of 0.36 and 0.5 mL/h, respectively. It was favorable to set a higher flow rate

for the outside solution for forming core-shell particles. This particle design should improve dispersity because it makes surface characteristics similar with those of L-100. In addition, physical stability of the drug phase can be improved if it is in the amorphous state, since the crystallization is often initiated from the surface.<sup>30,31</sup> This formulation was denoted GF/L-100. In a separate experiment, the GF/chloroform solution was used outside and the L-100/ethanol solution inside, with flow rates of 0.36 mL/h. In this case, the higher flow rate for the outside solution lowered electrospray stability due to lack in the intrinsic particle-formation ability for the outside solution as discussed later, and thus the same flow rates were employed. This formulation was denoted L-100/GF, and it was expected to possess a very large surface area of GF that may enhance the dissolution rate significantly. In both cases, the spray current was monitored to be in the range of 0.1–0.2  $\mu\text{A}$ .

**Morphology of Formulations.** Morphologies of all formulations were investigated by scanning electron microscopy (SEM) (S4800, Hitachi, Tokyo, Japan). Samples were sputter-coated using a platinum coater (E-1030 ion sputter, Hitachi, Tokyo, Japan) before the investigations.

Core-shell structures of the electrospray formulations were revealed using a confocal laser scanning microscope (CLSM) (LSM 510 Meta, Zeiss, Germany). Coumarin and Rhodamine B were added to the GF/chloroform and L-100/ethanol solutions at 100 and 10  $\mu\text{g}/\text{mL}$ , respectively, and the electrosprayed particles were dispersed in liquid paraffin with a mortar and pestle. It should be noted that most of the electrosprayed particles were too small to be observed with CLSM, and thus the particles captured in the confocal image are relatively large ones (i.e., not typical size) in the formulation.

Primal particle size of each formulation was determined by image analysis of the SEM pictures using Mac-View ver. 4 (Mountech, Tokyo, Japan). Three hundred particles were selected randomly from the image to obtain the Heywood diameter. Volume-mean diameter was used for the analysis.

Dynamic light-scattering analysis was also performed to evaluate possible aggregation of the particles on a Delsa Nano C Particle Analyzer (Beckman Coulter, Brea, CA, USA). The particles were suspended in simulated intestinal solution at pH 6.8 specified by the Japanese Pharmacopeia (JP-2 solution). The suspension was lightly sonicated prior to the measurements. A scattering angle of 165° and room temperature were used for the measurements. Mean particle size was calculated using the cumulant method.

**X-ray Powder Diffraction (XRPD).** Crystallinity of the formulations was investigated using a Rint-Ultima XRPD system (Rigaku Denki, Tokyo, Japan) with Cu K $\alpha$  radiation. The voltage and current were 40 kV and 40 mA, respectively. The sample was loaded on a glass plate, and the surface was carefully smoothed. Data were collected from 5° to 30° (2 $\theta$ ) at a scan rate of 2°/min for crystalline GF, and 0.5°/min for other formulations.

**Differential Scanning Calorimetry (DSC).** DSC experiments were performed on a Mettler Toledo DSC823° (Mettler Toledo, Greifensee, Switzerland), which was periodically calibrated using high purity indium. Samples (3–5 mg) were investigated using aluminum-sealed pans at a heating rate of 10 °C/min. Dry nitrogen was used as the inert gas at a flow rate of 30 mL/min.

**In Vitro Dissolution Study.** The dissolution study ( $n = 2$ ) was conducted using JP-2 solution with or without 20 mM taurocholic acid sodium salt at room temperature. Ground formulations (3 mg as a GF equivalent) were dispersed in 100 mL of

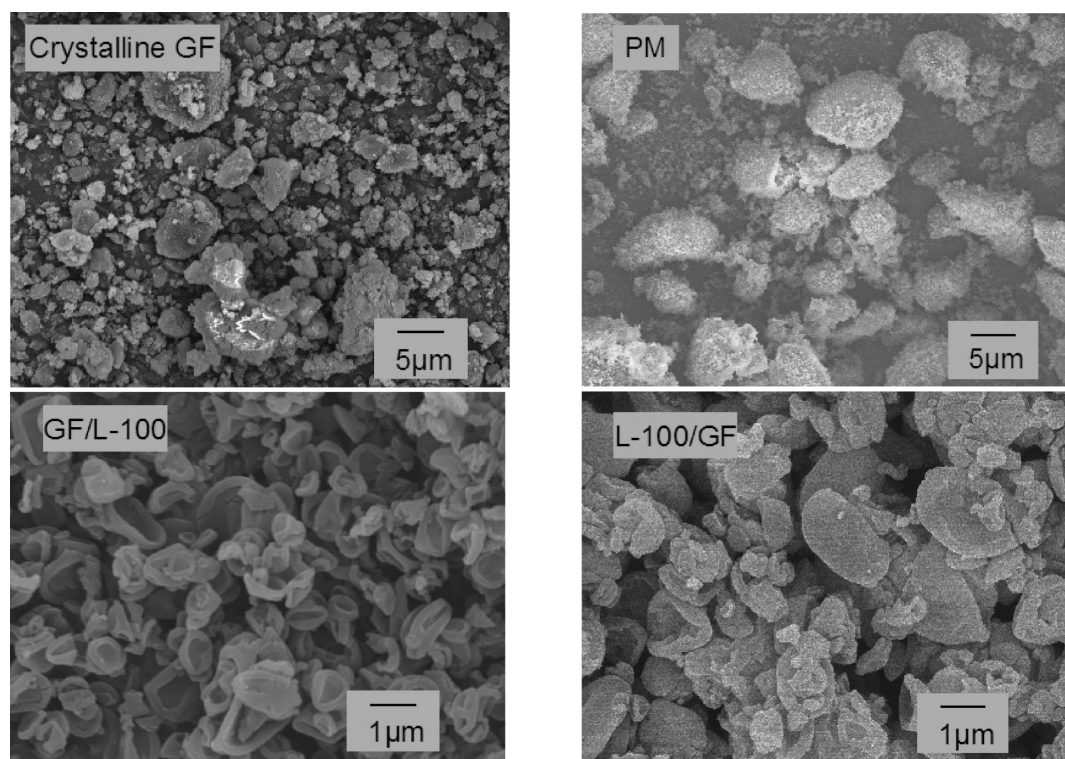


Figure 2. SEM images of the formulations.

Table 1. Physicochemical Characteristics of Formulations

formulation	crystal	PM	GF/L-100	L-100/GF
particle size <sup>a</sup> (µm)	-	-	0.84 ± 0.24	1.17 ± 0.39
particle size <sup>b</sup> (µm) (PI <sup>c</sup> )	2.47 (0.78)	1.97 (0.70)	1.86 (0.63)	2.70 (0.94)
GF content (%)	100	21.7	21.8	44.2
crystallinity <sup>d</sup> (%)	100	24.8	0	69.3

<sup>a</sup> Obtained from SEM image of samples. <sup>b</sup> Obtained by DLS measurement. <sup>c</sup> Polydispersity index. <sup>d</sup> Calculated from melting enthalpy.

medium under stirring with a magnetic stirrer. Aliquots were taken at fixed time intervals, and then filtered using a syringe filter with a pore size of 0.45 µm. Quantification of GF was performed by HPLC with a YMC-Pack Pro C18 column (150 mm × 2.0 mm i.d., YMC, Kyoto, Japan) at a flow rate of 0.2 mL/min. The mobile phase consisted of a mixture of acetonitrile and water at a ratio of 40/60 (v/v). Injection volume and the detection wavelength were 2 µL and 291 nm, respectively. Measurements were made in the concentration range from 2 to 100 µg/mL. Data were presented as mean ± standard deviation (SD).

**Oral Administration Study.** All experiments in rats were approved by the Ethical Review Committee of Setsunan University. Seven-week-old male Sprague–Dawley rats (weight: ca. 220 g) were fasted for 24 h with free access to water before experiments ( $n = 4$ ). Each formulation was dispersed in aqueous methylcellulose solution (0.1% w/v) at a concentration of 3 mg/mL as a GF equivalent. The dispersion was administered orally to rats in a single administration without anesthesia using a feeding needle at a volume of 2.5 mL of the dispersion per kg of body weight. Blood samples (0.8 mL) were taken from the jugular vein at predetermined time intervals under ether anesthesia. The blood was mixed with heparin and centrifuged at 5,000 rpm for 5

min at 4 °C to obtain plasma samples, which were stored at −20 °C until analysis.

Intravenous administration of GF was conducted to provide a bioavailability reference. Seven-week-old male Sprague–Dawley rats in the fed state were used. GF was dissolved in a mixture of DMSO and saline solution (1:9 v/v) at a concentration of 1.0 mg/mL. The drug solution was injected intravenously into the rats through the jugular vein under ether anesthesia at a volume of 0.75 mL/kg. Blood samples (0.8 mL) were taken from another jugular vein at predetermined time intervals under ether anesthesia. Plasma samples were obtained from the blood by means of the same procedure described above.

Drug concentrations in plasma were analyzed by HPLC. Plasma samples (0.1 mL) were mixed with 0.9 mL of acetonitrile. The mixture was shaken for 10 min, and the supernatant (0.8 mL) was collected after centrifugation at 15,000 rpm for 20 min (himac CF15R, HITACHI, Tokyo, Japan). After removal of the solvent under vacuum at 40 °C, residues were dissolved in 0.15 mL of a mixture of phosphate-buffered solution (50 mM, pH 2.5) and acetonitrile (65:35 v/v), which was used as a mobile phase as well. J'sphere ODS-H80 (75 mm × 4.6 mmID, YMC, Kyoto, Japan) was used as a column at 50 °C. Injection volume and flow rate were 50 µL and 1.0 mL/min, respectively. GF was detected using a fluorescence detector at an excitation wavelength of 303 nm and an emission wavelength of 428 nm with an 18 nm bandwidth. Measurements were made in the concentration range from 2.5 to 500 ng/mL.

**Data Analysis of Animal Studies.** Moment analysis was performed to estimate pharmacokinetic parameters. The area under the plasma concentration–time curve (AUC) from 0 to infinity was calculated by numerical integration using a linear trapezoidal formula and extrapolation to infinity on the basis of a single-exponential equation. Dose-corrected AUC after



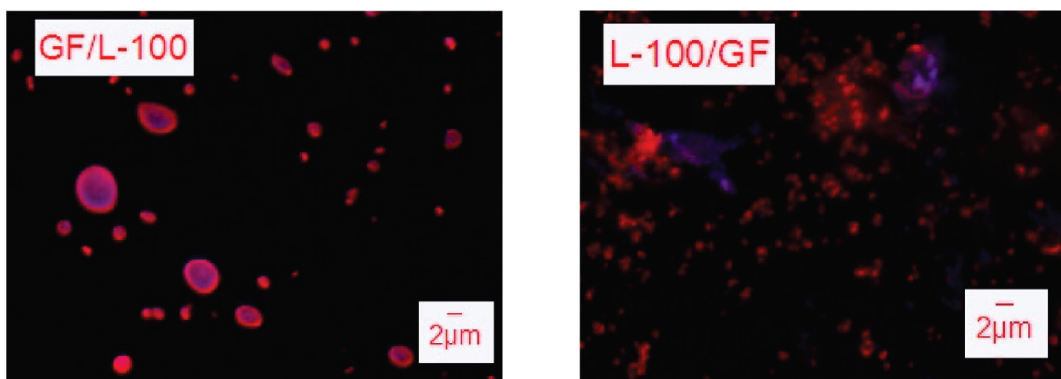


**Figure 3.** Confocal images of the electro spray formulations. The red and blue colors indicate the L-100 and GF phases, respectively.

intravenous administration of GF was used to calculate oral bioavailability. Data were presented as mean  $\pm$  standard deviation (SD) for individual groups. Statistical significance was assessed using the unpaired Student's *t* test; *p* values of 0.05 or less were considered significant.

## RESULTS AND DISCUSSION

**Particle Morphology.** SEM images (Figure 2) revealed that crystalline GF had irregular size and shape. The size of most particles was smaller than a few micrometers, however, large aggregations were found as well. For PM, large L-100 particles were found with adsorbed GF particles. The GF/L-100 particles had cavities on the surface, which is typical morphology of polymer particles prepared by drying droplets.<sup>32,33</sup> This can be explained by the formation of a polymeric skin layer on the droplet surface at an early stage of drying, followed by shrinkage due to removal of the solvent inside. The mean particle size obtained by the image analysis was smaller than 1  $\mu\text{m}$  (Table 1). The particle size of L-100/GF formulation was slightly larger than that of GF/L-100, and the adhesion force between L-100/GF particles appeared to be stronger than that between GF/L-100 particles.

Particle sizes obtained from the DLS measurements are presented in Table 1, which should take into account aggregation behavior. The particle size obtained in this analysis was slightly larger than that obtained by the image analysis, presumably due to aggregation of particles.

The confocal image of the GF/L-100 particles (Figure 3) revealed that the core-shell structure was obtained successfully, while in the case of L-100/GF particles, either phase seemed to exist homogeneously (i.e., the core-shell structure could not be formed). Note that the electro spray could not be performed with GF solution alone because of its low viscosity, which is probably related to this observation. In other words, intrinsic particle-formation ability seemed to be required for the outer solution for forming core-shell particles. As a result, GF and L-100 might form homogeneous particles or form particles individually. The SEM picture of L-100/GF indicated two types of particles: the caved and grain ones. The former was probably composed primarily of L-100, whereas the latter was of GF.

**Crystallinity.** The X-ray powder diffraction pattern of each formulation is shown in Figure 4. Sharp diffraction peaks were observed for both crystalline GF and PM. However, the baseline of PM indicated a decrease in crystallinity because the intensity of the halo pattern was stronger than expected due to the presence

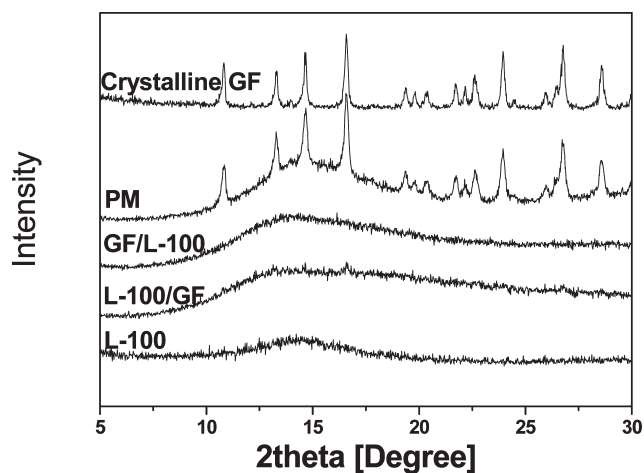


**Figure 4.** X-ray diffraction patterns of L-100 and formulations.

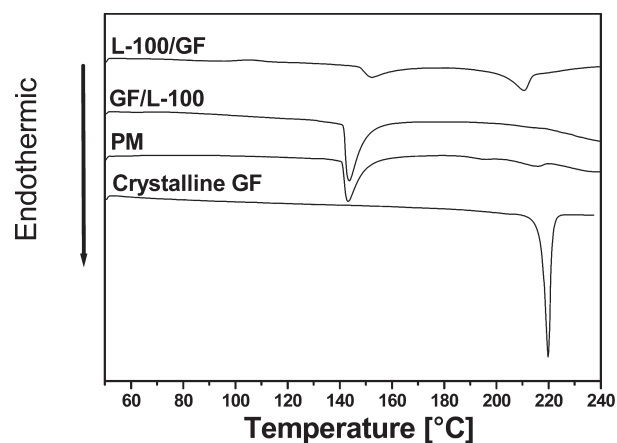


**Figure 5.** DSC curves of formulations. The heating rate was 10  $^{\circ}\text{C}/\text{min}$ .

of L-100. For the electro spray formulations, diffraction peaks were seldom observed. Note that the micro/nanosizing should contribute to the decrease in intensity of the diffraction peaks, and thus X-ray analysis may underestimate crystallinity of the electro spray formulations.

Figure 5 shows DSC curves of each formulation. A clear melting endothermic peak was observed for crystalline GF at 220  $^{\circ}\text{C}$ . Although no thermal event was observed for L-100 in the

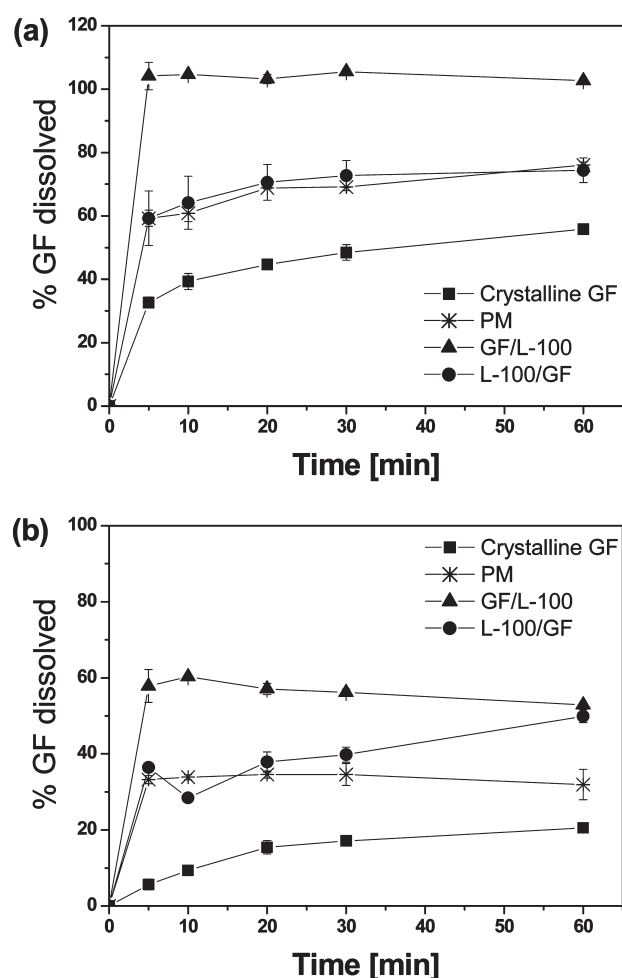


**Figure 6.** *In vitro* dissolution profiles of formulations in JP-2 solution (a) with or (b) without 20 mM taurocholic acid.

temperature range presented, endothermic peak appeared at about 140 °C for formulations that contain both L-100 and GF. Because the X-ray diffraction patterns were identical just above and below this peak (data not shown), the origin of this peak is unclear. However, it should be due to interaction between GF and L-100. Interestingly, melting enthalpy was very small for PM in spite of distinct peaks in the X-ray analysis. Melting enthalpy-based crystallinity was estimated to be 25%. In contrast, melting enthalpy for the L-100/GF formulation was relatively large, although peaks were hardly observed in the XRPD analysis. The crystallinity was estimated to be 69%. A possible explanation for this contradiction is that silent structural change including crystallization occurred during the heating process. For GF/L-100, almost complete amorphization was achieved. In addition, successful coating of the particle might improve physical stability of the amorphous GF, since recent studies on amorphous formulations suggest that crystallization can proceed from the surface of the formulation.<sup>30,31</sup>

***In Vitro* Dissolution Studies.** The dissolution profile of each formulation is shown in Figure 6. Although addition of taurocholic acid did not alter order of dissolution rate of the formulations, it did cause an increase in dissolution rate by *ca.* 1.5-to-2-fold for all cases. The dissolution of crystalline GF was slowest in both cases, whereas that of PM was increased, presumably because of promotion of the dispersion process in the presence

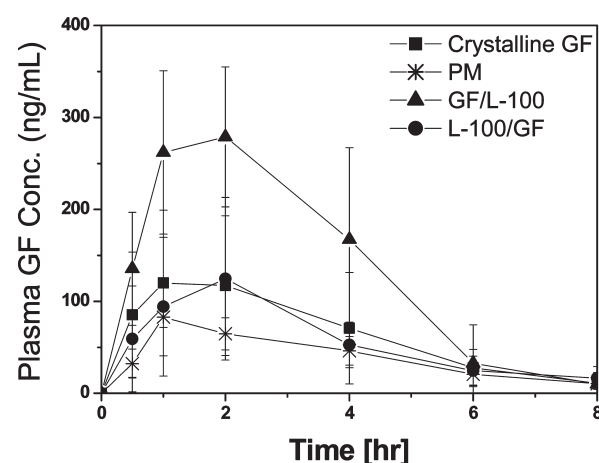


**Figure 7.** Plasma GF concentration–time profiles in the oral absorption study (7.5 mg/kg,  $n = 4$ ) using fasted rats.

of L-100 and a decrease in crystallinity. The dissolution behavior of L-100/GF was similar to that of PM, which agreed with the CLMS observation that showed L-100/GF was simple homogeneous formulation. Significant improvement in dissolution rate was observed for GF/L-100 formulation, and complete dissolution was achieved within 5 min in the presence of taurocholic acid. This effect was elucidated by nanosizing, improvement in dispersity, and complete amorphization.

**Oral Administration Study.** Figure 7 shows plasma concentration–time profiles of GF after oral administration of each formulation to rats. Oral bioavailability of GF was estimated to be  $13.2 \pm 7.4\%$  (mean  $\pm$  SD,  $n = 4$ ) when the drug was administered in crystalline form. Bioavailability of PM was constantly low ( $8.64 \pm 1.3\%$ ), indicating that L-100 minimally influenced oral absorption of GF, although there was not statistically significant difference. The formulation-dependent enhancement of drug absorption was not observed for L-100/GF (bioavailability:  $12.3 \pm 6.8\%$ ). In contrast, when GF cores were coated with L-100 shells (GF/L-100), oral absorption of GF was significantly enhanced, and the bioavailability was estimated to be  $27.1 \pm 10.2\%$ , which had statistically significant difference from that of PM. Moreover, this bioavailability was almost identical with that obtained with a GF DMSO/water solution ( $29.6 \pm 10.2\%$ ), which indicated that the dissolution problem, which is known as the rate-limiting step in the absorption of GF, was almost overcome by the core–shell formulation.

**Future Perspective of Electrospray Technology.** Current data indicate that the coaxial electrospray formulation has great potential to improve oral absorption of poorly water-soluble drugs. In addition to the advantages of electrospray deposition described in the Introduction, use of the coaxial nozzle allows greater variation in particle design strategies, because surface characteristics can be designed apart from the composition in the core phase. The dramatic increase in dissolution rate for the GF/L-100 formulation was partially explained by the increased dispersity resulting from shielding of GF from the particle surface. Moreover, physical stability may be improved significantly by coating the particle with excipients, because crystallization can occur from the particle surface under some conditions. Thus, various formulation strategies become possible using this novel formulation technology. Note that the electrospray with a single nozzle is a low throughput process which does

not seem to be suitable for industrial production. One possible solution is to use multinozzle systems, since the productivity linearly increases with the nozzle numbers. Further investigation on the scale-up of the instrument is required for industrial use of this technology.

## CONCLUSIONS

Coaxial electrospray formulations of griseofulvin were prepared using Eudragit L-100 as a polymeric excipient. The electrospray particles had a diameter around 1  $\mu\text{m}$ . The core-shell particles were obtained by using L-100 for the outer phase and GF for the inner one. However, GF and L-100 existed homogeneously when GF solution was used for outside and L-100 for inside. Although complete amorphization was achieved for the former particles, only a decrease in crystallinity was observed for the latter case. *In vitro* dissolution and *in vivo* oral absorption studies revealed that the formulation composed of GF core and L-100 shell exhibited significant improvement in dissolution and absorption behaviors, presumably because of a reduction in the particle size, improvement in dispersity, and complete amorphization. Coaxial electrospray has demonstrated potential as a novel formulation technology for enhancing oral absorption of poorly water-soluble drugs.

## AUTHOR INFORMATION

### Corresponding Author

\*K.K.: National Institute for Materials Science, Biomaterials Center, 1-1 Namiki, Tsukuba, Ibaraki 305-0044, Japan; e-mail, kawakami.kohsaku@nims.go.jp; phone, 81-29-860-4424; fax, 81-29-860-4714. S.S.: Faculty of Pharmaceutical Sciences, Setsunan University, 45-1 Nagaotoge-cho, Hirakata, Osaka 573-0101, Japan; e-mail, sakuma@pharm.setsunan.ac.jp; phone, 81-72-866-3124; fax, 81-72-866-3126.

## ACKNOWLEDGMENT

The authors are grateful to Mettler-Toledo for the use of the DSC 823e system. This work was supported by The Cosmetology Research Foundation and in part by World Premier International Research Center (WPI) Initiative on Materials Nanoarchitectonics, MEXT, Japan.

## REFERENCES

- (1) Lipinski, C. A.; Lombardo, F.; Dominy, B. W.; Feeney, P. J. Experimental and computational approaches to estimate solubility and permeability in drug discovery and development settings. *Adv. Drug Delivery Rev.* **1997**, *23*, 3–25.
- (2) Hann, M. M.; Oprea, T. I. Pursuing the leadlikeness concept in pharmaceutical research. *Curr. Opin. Chem. Biol.* **2004**, *8*, 255–263.
- (3) Zhang, M.; Wilkinson, B. Drug discovery beyond the ‘rule-of-five’. *Curr. Opin. Biotechnol.* **2007**, *18*, 478–488.
- (4) Vistoli, G.; Pedretti, A.; Testa, B. Assessing drug-likeness—what are we missing? *Drug Discovery Today* **2008**, *13*, 285–294.
- (5) Lawrence, M. J.; Rees, G. D. Microemulsion-based media as novel drug delivery systems. *Adv. Drug Delivery Rev.* **2000**, *45*, 89–121.
- (6) Kawakami, K.; Yoshikawa, T.; Moroto, Y.; Kanaoka, E.; Takahashi, K.; Nishihara, Y.; Masuda, K. Microemulsion formulation for enhanced absorption of poorly water-soluble drugs. I. Prescription design. *J. Controlled Release* **2002**, *81*, 65–74.
- (7) Kawakami, K.; Yoshikawa, T.; Hayashi, T.; Nishihara, Y.; Masuda, K. Microemulsion formulation for enhanced absorption of poorly

water-soluble drugs. II. *In vivo* study. *J. Controlled Release* **2002**, *81*, 75–82.

- (8) Pouton, C. W.; Porter, C. J. H. Formulation of lipid-based delivery systems for oral administration: Materials, methods and strategies. *Adv. Drug Delivery Rev.* **2008**, *60*, 625–637.

- (9) Hancock, B. C.; Zografi, G. Characteristics and significance of the amorphous state in pharmaceutical systems. *J. Pharm. Sci.* **1997**, *86*, 1–12.

- (10) Serajuddin, A. T. M. Solid dispersion of poorly water-soluble drugs: early promises, subsequent problems, and recent breakthroughs. *J. Pharm. Sci.* **1999**, *88*, 1058–1066.

- (11) Yu, L. Amorphous pharmaceutical solids: preparation, characterization and stabilization. *Adv. Drug Delivery Rev.* **2001**, *48*, 27–42.

- (12) Breitenbach, J. Melt extrusion: from process to drug delivery technology. *Eur. J. Pharm. Biopharm.* **2002**, *54*, 107–117.

- (13) Merisko-Liversidge, E.; Liversidge, G. G.; Cooper, E. R. Nano-sizing: a formulation approach for poorly-water-soluble compounds. *Eur. J. Pharm. Sci.* **2003**, *18*, 113–120.

- (14) Rabinow, B. E. Nanosuspensions in drug delivery. *Nat. Rev. Drug Discovery* **2004**, *3*, 785–796.

- (15) Wu, Y.; Loper, A.; Landis, E.; Hettrick, L.; Novak, L.; Lynn, K.; Chen, C.; Thompson, K.; Higgins, R.; Batra, U.; Shelukar, S.; Kwei, G.; Storey, D. The role of biopharmaceutics in the development of a clinical nanoparticle formulation of MK-0869: a beagle dog model predicts improved bioavailability and diminished food effect on absorption in human. *Int. J. Pharm.* **2004**, *285*, 135–146.

- (16) Kesiosoglou, F.; Panmai, S.; Wu, Y. Nanosizing — Oral formulation development and biopharmaceutical evaluation. *Adv. Drug Delivery Rev.* **2007**, *59*, 631–644.

- (17) Kawakami, K. Current Status of Amorphous Formulation and Other Special Dosage Forms as Formulations for Early Clinical Phases. *J. Pharm. Sci.* **2009**, *98*, 2875–2885.

- (18) Huang, Z. M.; Zhang, Y. Z.; Kotaki, M.; Ramakrishna, S. A review on polymer nanofibers by electrospinning and their applications in nanocomposites. *Compos. Sci. Technol.* **2003**, *63*, 2223–2253.

- (19) Agarwal, S.; Wendorff, J. H.; Greiner, A. Use of electrospinning technique for biomedical applications. *Polymer* **2008**, *49*, 5603–5621.

- (20) Ding, L.; Lee, T.; Wang, C. Fabrication of monodispersed Taxol-loaded particles using electrohydrodynamic atomization. *J. Controlled Release* **2005**, *102*, 395–413.

- (21) Chakraborty, S.; Liao, I.; Adler, A.; Leong, K. W. Electrohydrodynamics: A facile technique to fabricate drug delivery systems. *Adv. Drug Delivery Rev.* **2009**, *61*, 1043–1054.

- (22) Valo, H.; Peltonen, L.; Vehviläinen, S.; Karjalainen, M.; Koshtainen, R.; Laaksonen, T.; Hirvonen, J. Electrospray encapsulation of hydrophilic and hydrophobic drugs in poly(L-lactic acid) nanoparticles. *Small* **2009**, *5*, 1791–1798.

- (23) Ciach, T. Microencapsulation of drugs by electro-hydro-dynamic atomization. *Int. J. Pharm.* **2006**, *324*, 51–55.

- (24) Loscertales, I. G.; Barrero, A.; Guerrero, I.; Cortijo, R.; Marquez, M.; Gañán-Calvo, A. M. Micro/nano encapsulation via electrified-coaxial liquid jets. *Science* **2002**, *295*, 1695–1698.

- (25) López-Herrera, J. M.; Barrero, A.; López, A.; Loscertales, I. G.; Márquez, M. Coaxial jets generated from electrified Taylor cones. Scaling laws. *J. Aerosol Sci.* **2003**, *34*, 535–552.

- (26) Chen, H.; Zhao, Y.; Song, Y.; Jiang, L. One-step multicomponent encapsulation by compound-fluidic electrospray. *J. Am. Chem. Soc.* **2008**, *130*, 7800–7801.

- (27) Hwang, Y. K.; Jeong, U.; Cho, E. C. Production of uniform-sized polymer core-shell microcapsules by coaxial electrospraying. *Langmuir* **2008**, *24*, 2446–2451.

- (28) Wu, Y.; Yu, B.; Jackson, A.; Zha, W.; Lee, L. J.; Wyslouzil, B. E. Coaxial electrohydrodynamic spraying: A novel one-step technique to prepare oligodeoxynucleotide encapsulated lipoplex nanoparticles. *Mol. Pharmaceutics* **2009**, *6*, 1371–1379.

- (29) Zhang, S.; Kawakami, K. One-step preparation of chitosan solid nanoparticles by electrospray deposition. *Int. J. Pharm.* **2010**, *397*, 211–217.

- (30) Wu, T.; Yu, L. Surface crystallization of indomethacin below Tg. *Pharm. Res.* **2006**, *23*, 2350–2355.
- (31) Wu, T.; Sun, Y.; Li, N.; de Villiers, M. M.; Yu, L. Inhibiting surface crystallization of amorphous indomethacin by nanocoating. *Langmuir* **2007**, *23*, 5148–5153.
- (32) Vehring, R. Pharmaceutical particle engineering via spray drying. *Pharm. Res.* **2008**, *25*, 999–1022.
- (33) Kawakami, K.; Sumitani, C.; Yoshihashi, Y.; Yonemochi, E.; Terada, K. Investigation of the dynamic process during spray-drying to improve aerodynamic performance of inhalation particles. *Int. J. Pharm.* **2010**, *390*, 250–259.